



RESEARCH ARTICLE

# Evaluation of the $\alpha$ -amylase inhibitory activity of *Euclea natalensis* extracts used in the treatment of diabetes mellitus: An experimental and *in silico* approach

Keagile Bati<sup>1,2\*</sup>, Phazha Bushe Baeti<sup>1,3</sup>, Goabaone Gaobotse<sup>1</sup> & Tebogo E. Kwape<sup>1</sup>

<sup>1</sup>Department of Biological Sciences and Biotechnology, Faculty of Sciences, Botswana International University of Science and Technology, Palapye, Botswana.

<sup>2</sup>Department of Biomedical Sciences, Faculty of Medicine, University of Botswana, Gaborone, Botswana.

<sup>3</sup>Department of Medical Laboratory Sciences, Faculty of Health Sciences, School of Allied Health Professions, University of Botswana, Gaborone, Botswana.

\*Email: keagilebt2@gmail.com



## ARTICLE HISTORY

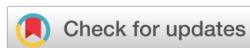
Received: 06 August 2023

Accepted: 21 December 2023

Available online

Version 1.0 : 22 May 2024

Version 2.0 : 25 May 2024



## Additional information

**Peer review:** Publisher thanks Sectional Editor and the other anonymous reviewers for their contribution to the peer review of this work.

**Reprints & permissions information** is available at [https://horizonepublishing.com/journals/index.php/PST/open\\_access\\_policy](https://horizonepublishing.com/journals/index.php/PST/open_access_policy)

**Publisher's Note:** Horizon e-Publishing Group remains neutral with regard to jurisdictional claims in published maps and institutional affiliations.

**Indexing:** Plant Science Today, published by Horizon e-Publishing Group, is covered by Scopus, Web of Science, BIOSIS Previews, Clarivate Analytics, NAAS, UGC Care, etc See [https://horizonepublishing.com/journals/index.php/PST/indexing\\_abstracting](https://horizonepublishing.com/journals/index.php/PST/indexing_abstracting)

**Copyright:** © The Author(s). This is an open-access article distributed under the terms of the Creative Commons Attribution License, which permits unrestricted use, distribution and reproduction in any medium, provided the original author and source are credited (<https://creativecommons.org/licenses/by/4.0/>)

## CITE THIS ARTICLE

Bati K, Baeti PB, Gaobotse G, Kwape TE. Evaluation of the  $\alpha$ -amylase inhibitory activity of *Euclea natalensis* extracts used in the treatment of diabetes mellitus: An experimental and *in silico* approach. Plant Science Today. 2024; 11(2): 750-761. <https://doi.org/10.14719/pst.2845>

## Abstract

Diabetes, a chronic metabolic disorder with increasing global prevalence, poses a significant public health concern, necessitating the development of safe and effective drugs. This study specifically assessed the inhibitory effects of *Euclea natalensis* leaf extracts on  $\alpha$ -amylase through *in vitro*, *in vivo*, and *in silico* methods. The extracts were sequentially obtained using solvents of graded polarity.  $\alpha$ -amylase inhibition studies were conducted through spectrophotometric methods, while *in vivo* assessments were performed using a starch tolerance test on rats. Molecular docking was carried out using Autodock 4.2.6, and SwissADME, along with ADMETlab 2.0, were employed to determine the drug-likeness and toxicity properties of the literature-mined compounds. The extracts demonstrated significant *in vitro* inhibition of  $\alpha$ -amylase, with the methanol extract exhibiting the highest percentage of inhibition at  $27\% \pm 4.2$ , followed by hexane and aqueous extracts at  $18\% \pm 2.5$  and  $18\% \pm 3.7$ , respectively. *In vivo*, the extracts lowered blood glucose levels, with acarbose reducing peak blood glucose levels by 42%, while both the aqueous and methanol extracts reduced it by 19% each after 30 min. The overall glucose-lowering effect, based on the area under the starch tolerance curve, ranked as follows: acarbose > methanol > aqueous > hexane > dichloromethane extract. Molecular docking identified 20(29)-lupene-3 $\beta$ -isoferulate C3 as the most promising compound with the lowest binding energy of -11.4 kcal/mol. Molecular dynamics revealed that C3 loses stability as it diverges from the active site. Additionally, while all other compounds passed the Lipinski drug-likeness criteria, 20(29)-lupene-3 $\beta$ -isoferulate C3 did not. Therefore, the present study suggests that *E. natalensis* exhibits antidiabetic properties through the inhibition of  $\alpha$ -amylase and may serve as a source of potential antidiabetic drug molecules.

## Keywords

Diabetes mellitus;  $\alpha$ -amylase; oral starch tolerance test; *Euclea natalensis*; phytochemicals

## Introduction

Diabetes mellitus is a chronic metabolic disorder that affects 500 million people, with global estimates projecting approximately 643 million cases by 2030 (1). It is characterized by chronic high blood sugar levels, attributed to

either the body's inability to produce insulin (Type 1 diabetes) or the body's inefficiency in using insulin (Type 2 diabetes) (2). Diabetes poses a significant public health concern due to associated complications, including cardiovascular disease, renal failure, blindness, and amputations. Traditional treatments for diabetes involve insulin injections and oral hypoglycemic medications (3), but these approaches have limitations due to side effects and can be expensive for poorly developing countries. In the United States alone, direct medical costs for managing diabetes surged from 116 billion USD in 2007 to 237 billion USD in 2017 (4), potentially placing an overwhelming burden on many countries. One widely used class of hypoglycemic drugs for managing type 2 diabetes is  $\alpha$ -amylase inhibitors. These drugs reduce postprandial hyperglycemia by limiting glucose absorption into the bloodstream.  $\alpha$ -amylase, a digestive enzyme, plays a role in converting complex carbohydrates into simpler sugars. In diabetes (5, 6), the activity of  $\alpha$ -amylase increases, leading to the rapid breakdown of carbohydrates and the subsequent release of glucose into the bloodstream. This process results in elevated blood sugar levels after a meal, termed post-prandial hyperglycemia—a hallmark of type 2 diabetes.

Therefore, drugs that inhibit the action of  $\alpha$ -amylase can slow down carbohydrate breakdown, ultimately reducing the release of glucose into the bloodstream and ensuring controlled blood glucose levels. Consequently,  $\alpha$ -amylase inhibitors play a critical role in the management of type 2 diabetes. However, synthetic inhibitors such as acarbose (7), miglitol (8), and voglibose (9) have limitations, including adverse effects and low bioavailability at target sites. Hence, there is a pressing need for new and effective  $\alpha$ -amylase inhibitors derived from natural sources. Given the high cost and notable side effects of glucose-lowering drugs (4, 10), many individuals turn to traditional medicinal plants to manage diabetes and its debilitating complications (11). Medicinal plants offer a holistic approach to diabetes management (10), and their readily availability (12) makes them a cost-effective alternative to modern medicine. Numerous medicinal plants have been identified as potential sources of  $\alpha$ -amylase inhibitors (13–16). These plants contain bioactive compounds that inhibit  $\alpha$ -amylase action, leading to a decrease in glucose release into the bloodstream. The bioprospecting of medicinal plants for  $\alpha$ -amylase inhibitors presents a promising strategy for diabetes treatment and has garnered scientific attention.

*Euclea natalensis* is an evergreen woody plant belonging to the Ebenaceae family, widely distributed in the forests of South Africa, Botswana, and other African nations. It has been extensively studied for its medicinal properties (17). The selection of this plant for the current study is based on its documented ethnopharmacological uses across various countries (17). *E. natalensis* is frequently employed in traditional medicine for the management of various conditions, including headaches, sexually transmitted infections, tuberculosis, skin

infections, and diabetes mellitus (17–19). Previous investigations have explored the antioxidant potential of the acetone root bark extract and ethanolic shoots extract. These studies found that their DPPH scavenging activity is comparable to that of vitamin C, as indicated by the inhibitory concentration providing 50% inhibition (IC<sub>50</sub>) (20). Additionally, the acetone root bark preparation demonstrated anti-diabetic properties by inhibiting the activities of  $\alpha$ -amylase and alpha-glucosidase (21). The ability of *E. natalensis* extracts to scavenge free radicals and inhibit carbohydrate-hydrolyzing enzymes supports the ethnopharmacological use of these extracts in managing diabetic complications. Therefore, the present study aims to assess the  $\alpha$ -amylase inhibitory effects of *E. natalensis* leaf extracts both *in vitro* and *in vivo* using normoglycemic rats. The reported compounds of *E. natalensis* will also be analysed through *in silico* studies to identify potent bioactive compounds that can be modelled into hypoglycemic drugs.

## Materials and Methods

### Plant collection and extraction

Matured leaves of *Euclea natalensis* were collected from Matlhakola village in Central Botswana and authenticated by Dr. M. Muzila at the University of Botswana herbarium (Voucher number: BAKW-01/2020). Subsequently, the leaves were cleaned with tap water, rinsed with distilled water, and left to dry in darkness at room temperature for 7 days. Using a household blender (Ottimo, South Africa), the dried leaves were ground into a fine powder. The powder was then sequentially extracted with different organic solvents in increasing polarity order. Approximately 2 kg of the powder was macerated in 3 L of non-polar n-hexane for 24 hrs with intermittent shaking at room temperature. The mixture was filtered using No. 1 Whatman filter paper, and the residue was subjected to two additional extractions with fresh liquid. The filtrates were combined, and the solvent was evaporated using a rotary evaporator at low pressure and temperature. Similar to the n-hexane extraction, the residue underwent extraction with dichloromethane: methanol (1:1, moderate polarity), 70% methanol (higher polarity), and water (highest polarity). The resulting four crude extracts were dried and stored at -20 °C for pending analysis.

### Experimental animals

40 Sprague Dawley rats, weighing between 150 and 180 g and aged 8 weeks, were housed in steel cages at the Botswana International University of Science and Technology (BIUST) animal house. The animal facility maintained a 12 hr dark/12 hr light cycle and a temperature of 24 ± 1 °C. Rats were provided with normal rodent feed (Epol, South Africa) and had unrestricted access to distilled water *ad libitum*. The animal study protocol was approved by the Ministry of Health and Wellness, with permit number HPDME 13/18/1.

### *In vitro* $\alpha$ -amylase inhibitory activity assay

To assess the impact of *Euclea natalensis* extracts on

$\alpha$ -amylase activity, the method described by Kamtekar (22) was employed to compare the inhibitory effects of the extracts at a high dose of 1 mg/mL (23). The various plant extracts were reconstituted in 20% DMSO, and 0.5 mL of 1 mg/mL of extracts or 0.5 mL of 50  $\mu$ g/mL of acarbose (positive control) were incubated with 0.5 mL of 0.5 mg/mL  $\alpha$ -amylase in 0.02 M sodium phosphate buffer (pH 6.9) and 6 mM sodium chloride at 37 °C for 10 min. Subsequently, 0.5 mL of 1% starch, prepared in the same buffer, was added, and the contents were further incubated at 37 °C for 30 min. Following this, 1 mL of dinitro salicylic acid (DNS) was added to halt the reaction, and the mixture was boiled for 5 min before being diluted to 5 mL with distilled water. Absorbance at 540 nm was determined using a Spec200E UV-Vis spectrophotometer (ThermoFisher Scientific, USA). The vehicle control used was 20% DMSO, and blanks for each extract were created by mixing all the above components but replacing the enzyme solution with buffer. The absorbance of blanks was subtracted from the absorbance of samples to eliminate bias brought about by the color of the extracts. The percentage inhibition was calculated as a percentage of the vehicle control, assuming 100% hydrolysis of starch in the absence of any inhibitor.

$$\text{Percentage inhibition} = \frac{\text{Abs(control)} - \text{Abs (sample)}}{\text{Abs(control)}} \times 100$$

.....Eqn. 1

#### Oral starch tolerance test (OSTT)

Oral starch tolerance tests were conducted as previously described (19). In summary, 30 fasted normoglycemic rats meeting the criteria—weighing between 160 and 180 g, aged 8 weeks, and having fasting blood glucose levels below 5.6 mmol/L (indicative of prediabetes cutoff) were divided into six groups of five each for statistical comparisons. The rats were orally administered with 100 mg/kg body weight of the extracts, chosen based on its efficacy in the oral glucose tolerance test (24).

Group 1: Starch solution + 2 mL Distilled water (Normal control)

Group 2: Starch solution + 50 mg/kg bw Acarbose (Positive control)

Group 3: Starch solution + 100 mg/kg bw Hexane (HEX) extract

Group 4: Starch solution + 100 mg/kg bw Dichloromethane-methanol 1:1 (DCM) extract

Group 5: Starch solution + 100 mg/kg bw 70% Methanol (MeOH) extract

Group 6: Starch solution + 100 mg/kg bw Aqueous (AQE) extract

Acarbose at 50 mg/kg bw (25) served as the positive control, while distilled water was used as the negative control. 15 min after treatment, the blood glucose level was measured (0 min), and the rats were orally administered a starch solution at a concentration of 3.0 g/kg body weight. Blood glucose levels (BG) were measured using a handheld glucometer (Accu-check Active, Germany) after

$$\text{AUC} \left( \frac{\text{mmol}}{\text{L}} \cdot \text{h} \right) = \frac{\text{BG}_0 + \text{BG}_{30} * 0.5}{2} + \frac{\text{BG}_{30} + \text{BG}_{60} * 0.5}{2} + \frac{\text{BG}_{60} + \text{BG}_{120} * 1}{2}$$

30, 60, and 120 min. The peak blood glucose (PBG) was determined by observing the blood glucose level during the mentioned time intervals, and the area under the curve (AUC) was calculated using the formula below:

.....Eqn. 2

Where BG stands for blood glucose levels at time intervals 0, 30, 60 and 120 min.

#### In silico studies

##### Ligands preparation

To identify the isolated or identified compounds in *Euclea natalensis* extracts, a comprehensive literature review was conducted, encompassing published articles up until 2021. The 14 compounds discovered during this investigation are presented as 2D structures in Table 1. The 3D structures of these 14 ligands were obtained as SDF files from PubChem (<https://pubchem.ncbi.nlm.nih.gov/>) and subsequently converted to PDB files using Discovery Studio. Subsequently, the ligands underwent further preparation through Autodock tools, which involved calculating Gasteiger charges and saving them as PDBQT files.

##### Protein preparation

The crystal structure of human intestinal amylase (1B2Y) in complex with acarbose was obtained from the RCSB Protein Data Bank (<https://www.rcsb.org/>). Using Discovery Studio, the protein structure was prepared by removing the bound acarbose, water molecules, heteroatoms, and chain B. Subsequently, the remaining chain A was further processed using Autodock tools, involving the addition of Kollman charges and polar hydrogens. The final structure was then saved in PDBQT format.

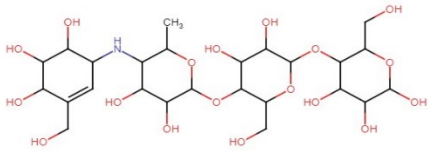
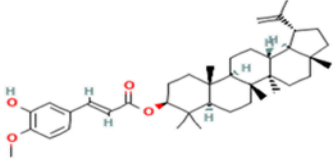
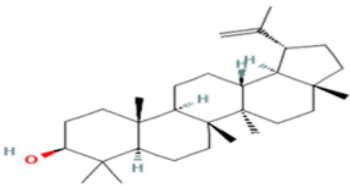
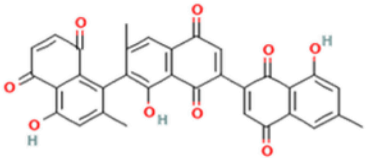
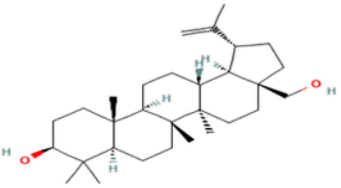
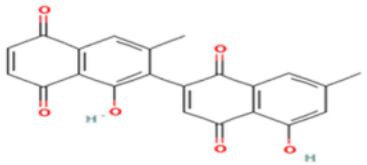
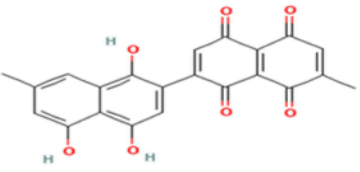
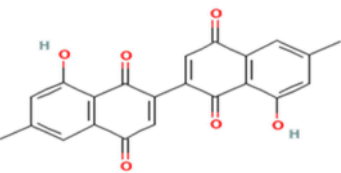
##### Molecular docking

The  $\alpha$ -amylase binding site residues were identified using Discovery Studio Visualizer, referencing the publication where 1B2Y was co-crystallized with acarbose, and the structure was deposited in the Protein Data Bank (PDB). Subsequently, a grid box was defined with coordinates  $x = 17.388$ ,  $y = 5.268$ , and  $z = 46.733$ , centered around the active site of  $\alpha$ -amylase, with grid sizes of  $60 \times 60 \times 60$  at 3.75 spacing. Molecular docking was performed with Autodock 4.2.6 (<https://autodock.scripps.edu/>) utilizing Lamarckian genetic algorithms. Compounds were assessed based on their binding affinities and the nature of molecular interactions with the protein. The ligands were individually docked with 100 cycles to identify the pose with the lowest binding affinity (kcal/mol).

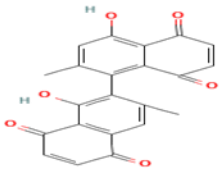
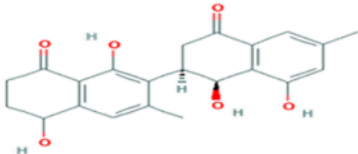
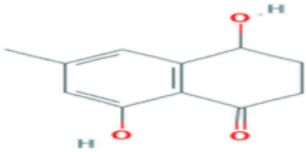
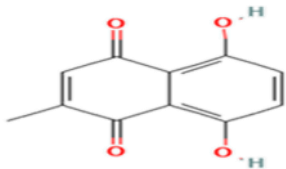
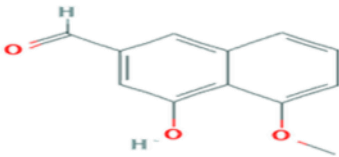
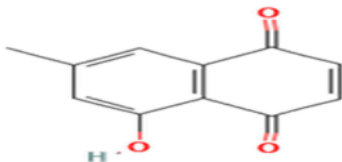
##### Molecular dynamic simulations

The Desmond module of the Schrödinger software was employed to conduct molecular dynamics simulation tests, aiming to analyze the conformational changes and stabilities of the top two best-amylase compound complexes with C2, C3, and the positive control Acarbose. The TIP3P model was utilized to determine the optimal docking poses of the ligands in association with  $\alpha$ -amylase

**Table 1.** Binding affinity scores and interactions of compounds with  $\alpha$ -amylase.

ID	Ligand	2D Structure	Affinity (kcal/mol)
	Acarbose		-11.2
C3	20(29)-lupene-3 $\beta$ -isoferulate		-11.4
C2	Lupeol		-9.9
C7	Galpinone		-9.4
C1	Betulin		-9.3
C10	Diospyrin		-8.6
C6	Euclanone		-8.4
C9	Neodiospyrin		-8.3
C5	Mamegakinone		-8.1

within an explicit orthorhombic periodic boundary box with a size of 10 Å. Using the built-in Desmond System

C4	Isodiospyrin		-7.9
C13	Octahydroeuclein		-7.2
C12	Shinanolone		-6.0
C8	Methylnaphthazarin		-5.8
C14	4-Hydroxy-5-methoxy-2-naphthaldehyde		-5.6
C11	7-Methyljuglone		-5.6

Builder tool, the simulated system was neutralized by adding the appropriate amounts of Na<sup>+</sup> and Cl<sup>-</sup>. The NPT ensemble, incorporating a Nose-Hoover thermostat and

barostat, was employed to maintain the temperature and pressure at 300 K and 1 bar, respectively. The OPLS-3e force field within Desmond's molecular dynamics module was utilized for running the simulation, and the runtime was set at 100 ns. Following the simulation runs, the trajectory files were examined using the Desmond simulation analysis module to calculate various structural parameters, such as the root mean square deviation (RMSD) and the root mean square fluctuation (RMSF)

#### ADME and drug-likeness analysis

The simplified molecular input line entry system (SMILES) for each compound was retrieved from PubChem and input into the SwissADME software (<http://www.swissadme.ch/>) to assess drug-likeness based on the

Lipinski parameters. Additionally, the absorption, distribution, metabolism, excretion, and toxicity (ADMET) properties were determined using ADMETLab 2.0 (<https://admetmesh.scbdd.com/>)

#### Statistical analysis

The results are presented as the mean ( $n = 3$ ) for *in vitro* studies and  $n = 5$  for *in vivo* studies, accompanied by the standard deviation (SD). Statistical significance was determined at  $p < 0.05$  using One-way analysis of variance (ANOVA) with Tukey-Kramer's range test. All statistical analyses and graphing were performed using GraphPad Prism version 9.0.

#### Results

##### *α*-amylase inhibition

The *in vitro* amylase inhibition was most pronounced with acarbose, exhibiting a percentage inhibition of  $49\% \pm 1.2$ ,

as depicted in Fig. 1. Following this, the MeOH extracts demonstrated a considerable inhibition at  $27\% \pm 4.2$ , while

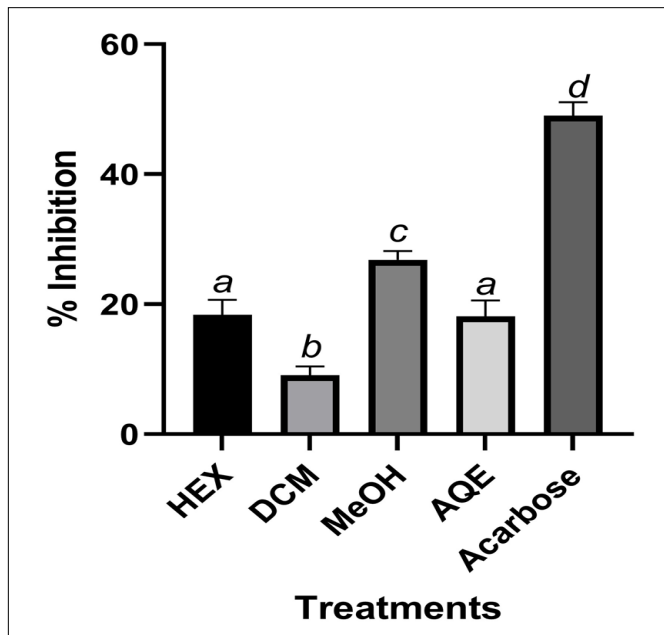


**Fig. 1.** Percentage inhibitory effect of *Euclea natalensis* leaf extracts on  $\alpha$ -amylase activity. Results are presented as mean ( $n = 3$ )  $\pm$  standard deviation (SD). Bars with the same letters (a, b, c, or d) are not significantly ( $p < 0.05$ ) different, while those with different letters are significantly ( $p < 0.05$ ) different. **HEX:** hexane extract; **DCM:** dichloromethane-methanol (1:1) extract; **MeOH:** 70% methanol extract; **AQE:** aqueous (water) extract.

HEX and AQE extracts showed inhibition levels of  $18\% \pm 2.5$  and  $18\% \pm 3.7$ , respectively. The lowest inhibition was observed with DCM at  $9\% \pm 0.8$ . All extracts were statistically different ( $p < 0.05$ ) from acarbose and from each other, except for HEX and AQE extracts, which were not significantly different ( $p < 0.05$ ) from each other.

#### Oral starch tolerance test

Fig. 2 illustrates the impact of the extracts on blood glucose levels following the administration of a starch solution to rats. The normal control (NC) exhibited a peak blood glucose level (PBGL) of 8.67 mmol/L and an area under the curve (AUC) of  $21 \pm 1.2$  mmol/L.min on the 2 hr starch tolerance curve. Within the 2 hr study duration, treatment with *Euclea natalensis* extracts and acarbose led to a reduction in PBGL and AUC. According to Table 1, acarbose reduced PBGL by 42%, while both AQE and MeOH

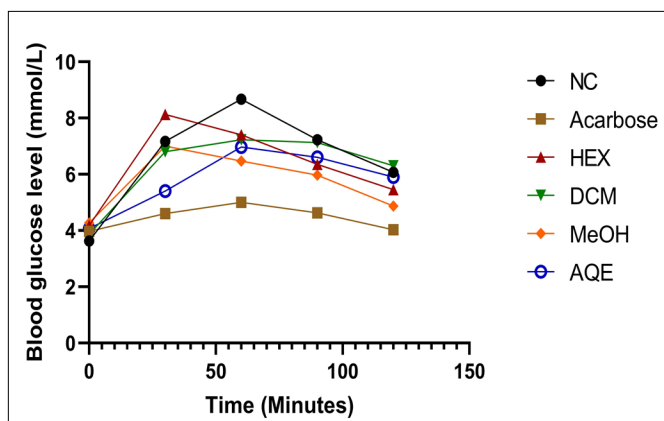


**Fig. 2.** Effects of *Euclea natalensis* leaf extracts on starch tolerance in normoglycemic rats. Results are presented as mean ( $n = 5$ ). **HEX:** hexane extract; **DCM:** dichloromethane-methanol (1:1) extract; **MeOH:** 70% methanol extract; **AQE:** aqueous (water) extract.

extracts reduced it by 19%. HEX extracts showed the lowest PBGL decrease. Acarbose achieved an AUC of  $13 \pm 0.3$ , compared to the normal control's AUC of  $21 \pm 1.2$  mmol/L.min, representing a 36% reduction, which exceeded the average for all extracts. Table 2 further

**Table 2.** Effects of treatments on peak blood glucose level (PBGL) and area under the curve (AUC) after starch loading in normoglycemic rats.

Treatment groups	PBGL (mmol/L)	% Change	AUC (mmol/L.min)	% Change
NC	9	-	$21 \pm 1.2$	-
Acarbose	5	42 <sup>a</sup>	$14 \pm 0.3$	36 <sup>a</sup>
HEX	8	6 <sup>b</sup>	$20 \pm 1.3$	8 <sup>b</sup>
DCM	7	17 <sup>c</sup>	$20 \pm 1.4$	6 <sup>b</sup>
MeOH	7	19 <sup>c</sup>	$19 \pm 0.1$	16 <sup>c</sup>
AQE	7	19 <sup>c</sup>	$19 \pm 0.6$	13 <sup>c</sup>

Mean with the same letters (a, b, c, or d) in a column are not significantly ( $p < 0.05$ ) different, while those with different letters are significantly ( $p < 0.05$ ) different. **HEX:** hexane extract; **DCM:** dichloromethane-methanol (1:1) extract; **MeOH:** 70% methanol extract; **AQE:** aqueous (water) extract.

reveals that acarbose was followed by MeOH, AQE, and HEX extracts, while DCM extracts showed the least reduction in the AUC of the starch tolerance curve. In terms of lowering AUC, there was no significant difference ( $p < 0.05$ ) between MeOH and AQE extracts, as well as between HEX and DCM extracts.

#### Molecular docking analysis

The search for phytochemicals isolated and identified from *Euclea natalensis* yielded 14 compounds, which were subjected to virtual screening using Autodock 4.2.6. The human  $\alpha$ -amylase (PDB: 1B2Y) co-crystallized with acarbose was re-docked to validate the protocol, and acarbose served as the positive control. Docking analysis revealed that acarbose binds to the active site of  $\alpha$ -amylase by forming hydrogen bonds with amino acid residues GLN63, HIS305, GLY306, ILE235, LYS200, ALA198, GLU233, ARG195, ASP197, and TRP59, as illustrated in Fig. 3 (a, c). It also engaged in Van der Waals and hydrophobic interactions, resulting in a binding energy of -11.2 kcal/mol, as shown in Table 1. The 14 bioactive compounds from *E. natalensis* interacted with the active site of  $\alpha$ -amylase, forming hydrogen bonds, Van der Waals forces, and hydrophobic forces, contributing to varying binding affinities. Among these, the bioactive compound 20(29)-lupene-3 $\beta$ -isoferulate C3 exhibited the lowest binding energy of -11.4 kcal/mol, surpassing that of acarbose, the clinically used drug. Fig. 3 (b, d) depicts the 3D structure (b) and 2D structure of 20(29)-lupene-3 $\beta$ -isoferulate C3 interacting with amino acids on the active site of  $\alpha$ -amylase via hydrogen bonding (GLY306, LYS200, HIS201), Van der Waals, and hydrophobic forces. Following this, Lupeol C2 exhibited a binding energy of -9.9 kcal/mol, forming one hydrogen bond with amino acid residue GLU233 (Fig. 3 e, g). Galpinone C7 demonstrated a binding energy of -9.4 kcal/mol, engaging in hydrogen bonding with GLN63 and HIS305. Betulin C1, although exhibiting hydrogen bonding, surprisingly had a high binding energy

of -9.3 kcal/mol. The compound with the least favourable binding energy was 7-Methyljuglone C11, with -5.6 kcal/mol.

#### Molecular dynamic simulation

The root mean square deviation (RMSD) values of the complex 1B2Y with acarbose did not exceed those of the backbone 1B2Y, and the fluctuations stabilized after 20 sec, indicating that acarbose formed a stable complex on the active site of the protein, as depicted in Fig. 3a.

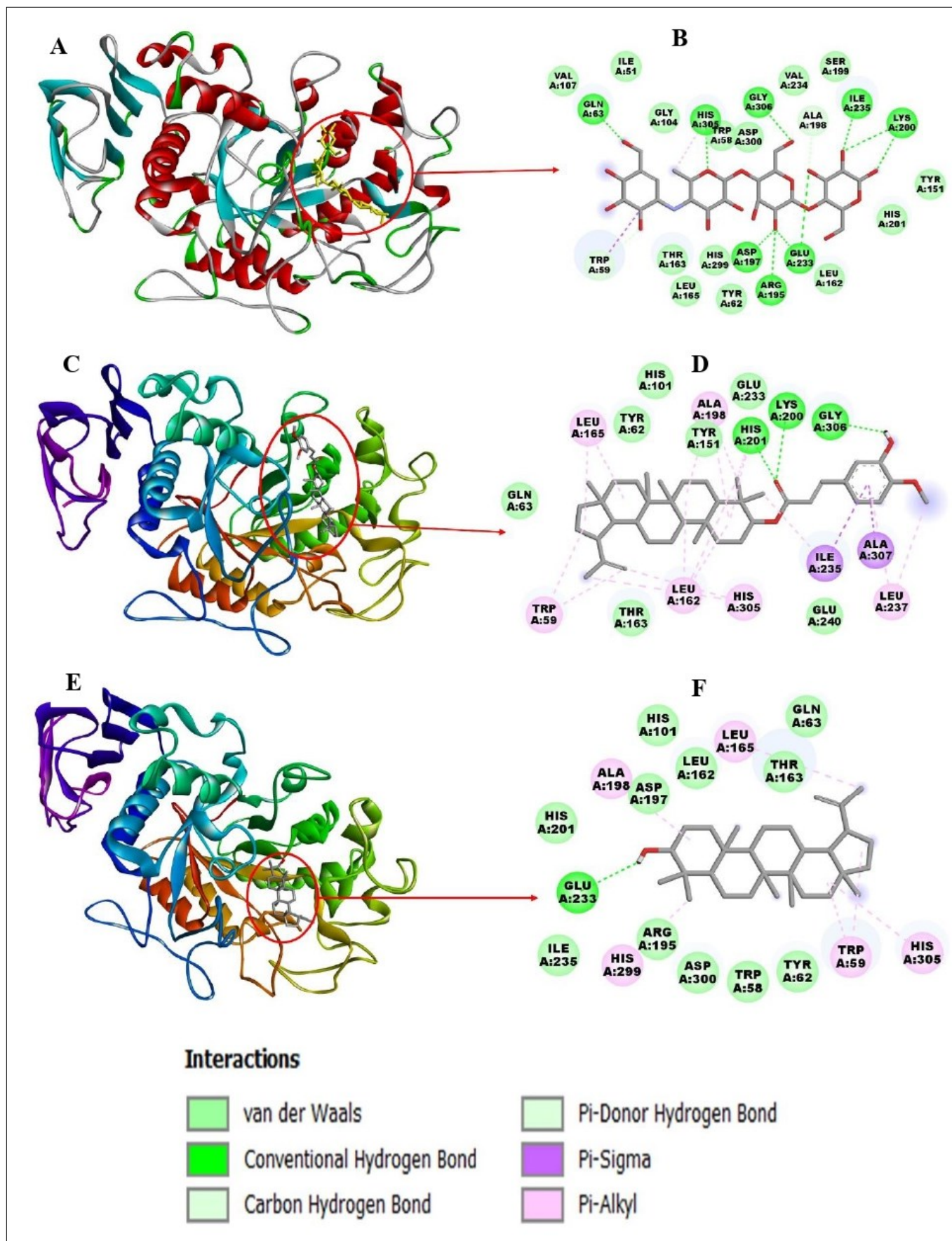


**Fig. 3.** Binding interactions of acarbose (a, c), 20(29)-lupene-3 $\beta$ -isoferulate C3 (b, d), lupeol C2 (e, g) and galpinone C7 (f, h) interacting with human  $\alpha$ -amylase (PDB: 1B2Y).

Concerning 1B2Y in complex with C2, the RMSD of the complex was larger, and after 50 sec, it lost stability as major fluctuations deviated from those of the protein backbone, as observed in Fig. 4c. The complex of 1B2Y with C3 initially showed RMSD values aligning well and not exceeding those of the backbone. However, after 43 sec, the RMSD deviated away from the backbone, suggesting

were assessed based on Lipinski's rule of 5, and the results are presented in Table 3. All the compounds met Lipinski's rule of 5, qualifying as druggable compounds, except for 20(29)-lupene-3 $\beta$ -isoferulate C3. This specific bioactive compound violated the Lipinski rules related to molecular weight (< 500 g/mol) and lipophilicity (LogP < 5), thus failing to meet the criteria for drug-likeness according to

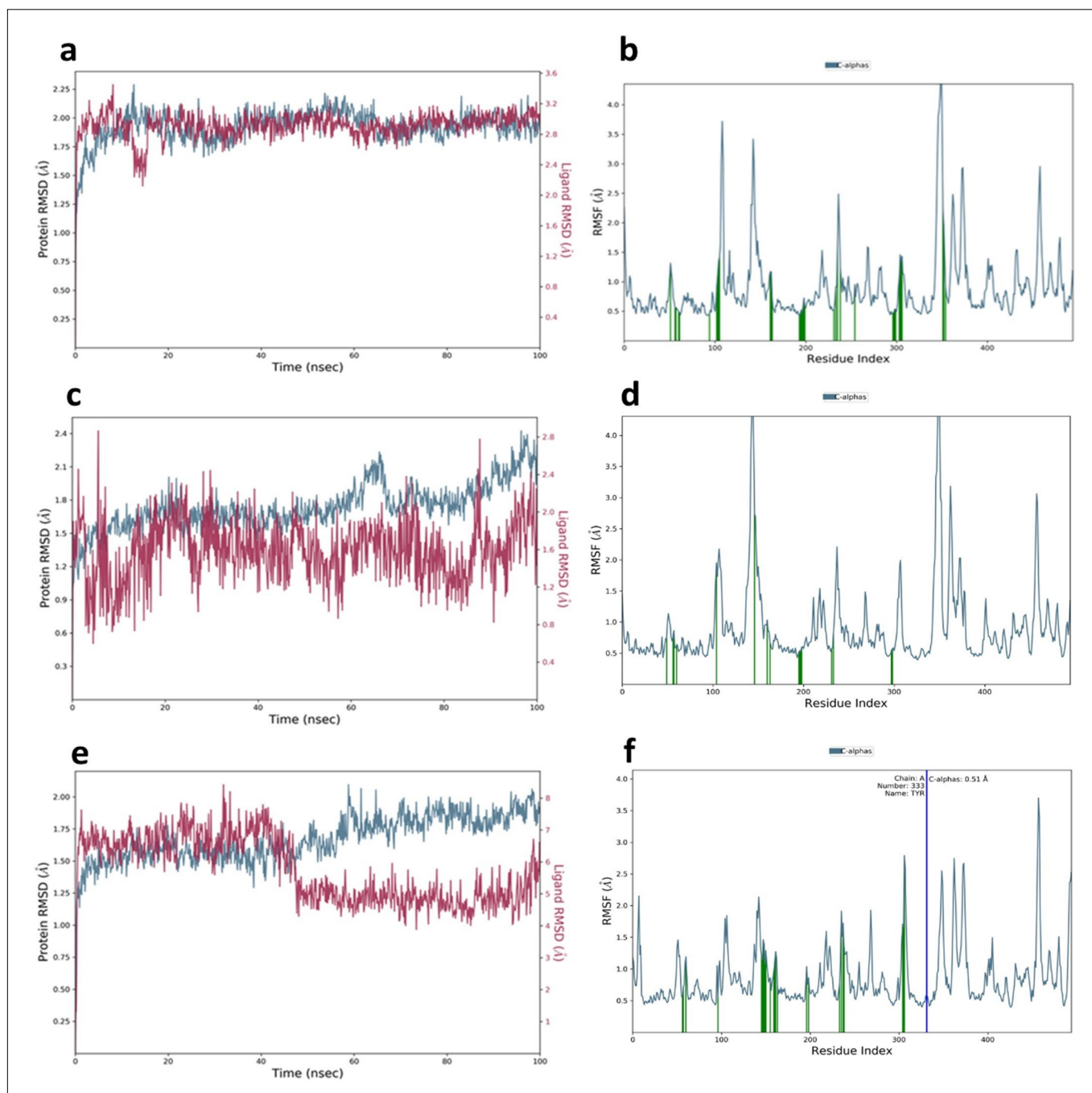


**Fig. 4.** Molecular dynamics simulations results of complexes; RMSD (a) and RMSF (b) of acarbose, compound C2 (c, d) and compound C3 (e, f).

that the compound was dispersing away from the active site, as seen in Fig. 4e. The root mean square fluctuation (RMSF), illustrating the impact of ligand binding on protein residues, was computed for all compounds and the control acarbose. The RMSF graphs demonstrate that the fluctuations in Fig. 4 (b, d, f) for acarbose, C2, and C3, respectively, interacted with residues of 1B2Y, exceeding 3.0 Å.

#### Analysis of drug-likeness of the compounds

The drug-likeness properties of the bioactive compounds

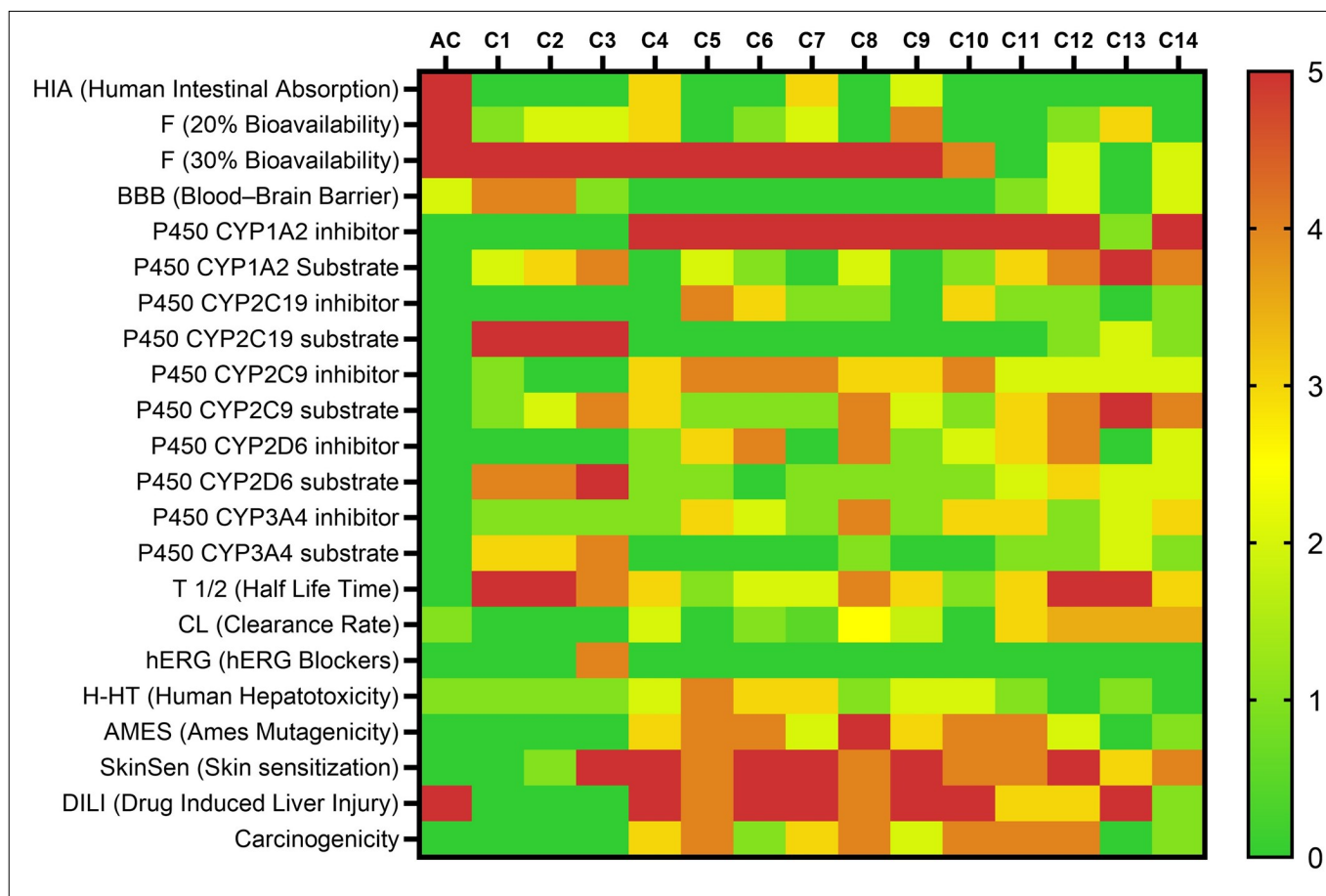
were assessed based on Lipinski's rule of 5.

#### Analysis of ADMET profiles of the compounds

The absorption, distribution, metabolism, excretion, and toxicity (ADMET) properties were evaluated *in silico* and are presented in Fig. 5. In comparison to acarbose, all the compounds exhibited moderate to excellent intestinal absorption and 20% bioavailability. With the exception of C1, C2, C3, and C13, most compounds interacted with and inhibited the P450 cytochrome CYP1A2, while C1, C2, and C3 were likely to be substrates of the P450 cytochrome

**Table 3.** Drug-likeness properties of *Euclea natalensis* phytochemicals.

ID	Compound name	Lipinski's Rule of 5					Drug-likeness
		Molecular weight (g/mol)	Lipophilicity (MLogP)	H-bond donors	H-bond acceptors	Rule violations	
		<500	<5	<5	<10	<2	
C1	Betulin	442.72	6.0	2	2	1	Yes
C2	Lupeol	426.72	6.92	0	1	1	Yes
C3	20(29)-lupene-3 $\beta$ -isoferulate	602.89	6.96	1	4	2	No
C4	Isodiospyrin	374.34	0.62	2	6	0	Yes
C5	Mamegakinone	374.34	0.62	2	6	0	Yes
C6	Euclanone	390.34	0.24	3	7	0	Yes
C7	Galpinone	560.51	0.31	3	9	1	Yes
C8	Methylnaphthazarin	204.18	0.01	2	4	0	Yes
C9	Neodiospyrin	374.34	0.62	2	6	0	Yes
C10	Diospyrin	374.34	0.62	2	6	0	Yes
C11	7-methyljuglone	188.18	0.59	1	3	0	Yes
C12	(R)-Shinanolone	192.21	0.76	2	3	0	Yes
C13	Octahydroeuclein	382.41	0.91	4	6	0	Yes
C14	4-Hydroxy-5-methoxy-2-naphthaldehyde	202.21	1.49	1	3	0	Yes

**Fig. 5.** Heatmap of ADMET properties of acarbose and *Euclea natalensis* phytochemicals. AC: acarbose, C1 – C14: phytocompounds of *E. natalensis*. 0: good and 5: bad/poor.

CYP2C19. Regarding excretion, all the compounds displayed moderate to good clearance rates and half-life times, except for C1, C2, C12, and C13, which exhibited extremely high half-lives. While some compounds showed moderate to a high degree of toxicity, C1 demonstrated safety with no hepatotoxicity, skin sensitization, mutagenicity, and carcinogenicity.

## Discussion

In this study, we evaluated the *in vitro* antidiabetic potential of *Euclea natalensis* leaf extracts based on the inhibition of the activity of one of the key carbohydrate-digesting enzymes,  $\alpha$ -amylase. This enzyme is implicated

in managing postprandial hyperglycemia in type 2 diabetic patients. The strategy of suppressing postprandial hyperglycemia through the inhibition of  $\alpha$ -amylase has led to the discovery of acarbose, a clinical drug with this mechanism (7, 26). The solvent extracts of *E. natalensis* demonstrated inhibition of  $\alpha$ -amylase activities, as depicted in Fig. 1. The highest inhibitory effect on  $\alpha$ -amylase activity was observed with MeOH extracts, significantly surpassing all other extracts and indicating superior  $\alpha$ -amylase inhibitory activity. The enzyme  $\alpha$ -amylase is found in saliva and the small intestines, secreted by the pancreas. It hydrolyzes the alpha-1,4-glycosidic bonds of starch's amylose and amylopectin components into oligosaccharides and disaccharides such as sucrose and maltose (27, 28). Inhibition of  $\alpha$ -amylase results in reduced availability of disaccharides, leading to decreased glucose absorption into the bloodstream (27). Our results align with the findings of Nkobole and colleagues (21), who reported that the acetone root bark extract of *E. natalensis* inhibited the enzymatic activity of  $\alpha$ -amylase.

After establishing the *in vitro* inhibition of  $\alpha$ -amylase by the extracts, we sought to determine whether this inhibition also occurred in live animals. We investigated the effects of the extracts on blood glucose levels in normoglycemic rats administered a starch solution, as depicted in Fig. 2. Administering the starch solution to normal rats resulted in an increase in blood glucose levels and a high area under the curve (AUC) in the 2 hr starch tolerance test, as presented in Table 2. Surprisingly, treatment with the extracts and acarbose led to a reduction in peak blood glucose levels (PBGL) and AUC in normoglycemic rats. While acarbose significantly lowered blood glucose levels more than all the extracts, the MeOH and AqE extracts exhibited the highest inhibitory effects among all other extracts, with no statistical difference ( $p < 0.05$ ) between the effects of MeOH and AqE extracts. The decrease in PBGL and AUC suggests that the extracts inhibited the enzyme  $\alpha$ -amylase *in vivo*, confirming the *in vitro* inhibitory effects. The inhibition of  $\alpha$ -amylase reduces glucose release and absorption in the small intestines, thereby suppressing postprandial glycemia. We hypothesize that bioactive compounds previously reported (19, 29) may be responsible for the observed inhibition of  $\alpha$ -amylase. Our results align with previous studies demonstrating the *in vivo* inhibition of  $\alpha$ -amylase using the starch tolerance test with plant extracts (30–32).

The *in vitro* and *in vivo* inhibitory effects of the extracts sparked an interest in understanding how the bioactive compounds interact with amylase at the molecular level. This was investigated using molecular docking, a molecular modelling technique that predicts how a protein interacts with a ligand and determines a stable conformation (33). Molecular docking has become a key tool in computer-aided drug discovery. In this study, 14 compounds from *E. natalensis* were subjected to molecular docking analysis. Among them, 20(29)-lupene-3 $\beta$ -isoferulate C3 exhibited the lowest binding energy of -11.4 kcal/mol, even lower than that of acarbose

(-11.2 kcal/mol). In molecular docking, a more negative binding energy indicates a more stable protein–ligand complex (34, 35). The stability of the complex is achieved through hydrogen bonding and electrostatic forces, both observed in our study. While acarbose formed hydrogen bonds with 10 amino acid residues on the active site of  $\alpha$ -amylase, 20(29)-lupene-3 $\beta$ -isoferulate C3 had hydrogen bonds with 3 amino acids. Despite having only 3 hydrogen bonds, the lowest binding energy of amylase - C3 may be attributed to the  $\delta$  and  $\pi$ -bonds formed with 8 amino acid residues. Overall, all compounds interacted with the protein, resulting in varying binding energies and types of interactions. The complexes with the highest docking scores, C2 and C3, were subjected to molecular dynamics simulations. The root mean square deviation (RMSD) values, depicting the stability of the complex over the analysis time frame (36), revealed that C2 and C3 complexes were not as stable as the complex with acarbose. C3 showed fluctuations that diverged significantly from the 1B2Y protein backbone, indicating that C3 loses stability and disperses away from the active site of the protein. Although the RMSD values of C2 in complex with 1B2Y were substantial, the divergence was not as significant as that of C3. The root mean square fluctuation (RMSF) was computed to analyse residual fluctuations over the simulation time (37). The RMSF showed fluctuations of more than 3.0 Å in all complexes, indicating higher flexibility (38). Our results align with a study by Oyewusi (39) where Withanolide A from the plant *Withania somnifera* exhibited strong and stable binding energies along with high flexibility, as indicated by RMSF.

In addition to molecular docking, the bioactive compounds were assessed for their potential to be developed into drugs. The evaluation of drug-likeness was based on Lipinski's Rule of Five, which comprises five properties determining the oral activity of a compound in humans (32). All compounds demonstrated druggable characteristics, except for 20(29)-lupene-3 $\beta$ -isoferulate C3, which violated Lipinski's rule regarding molecular weight ( $< 500$  g/mol) and the lipophilicity rule ( $\text{LogP} < 5$ ). While this finding suggests the potential for these bioactive compounds to be further developed into drugs, it is crucial to note that the ADMET profiles indicated potential toxicity for most of them, with the risk of causing liver injury, mutations, or interference with drugs metabolized by the P450 enzymes CYP1A2 and CYP2C19. It is noteworthy that compounds from other plants have been reported to interact with  $\alpha$ -amylase without exhibiting signs of toxicity (40, 41). For instance, in a chemoinformatics analysis for drug-likeness, Topotecan from the plant *Leucas ciliata* Benth inhibited  $\alpha$ -amylase with no apparent toxicity potential, satisfying Lipinski's Rule of Five for drug candidate molecules intended for oral administration (40).

## Conclusion

The present study successfully demonstrated the inhibitory effects of *Euclea natalensis* leaf extracts on  $\alpha$ -amylase through both *in vitro* and *in vivo* approaches.

Molecular docking and dynamic simulations with the identified bioactive compounds revealed a strong binding affinity, suggesting their potential for drug development. However, further research is warranted to isolate and thoroughly evaluate the pharmacological value of these bioactive compounds. Human studies are also necessary to determine whether similar results can be obtained in human subjects.

## Acknowledgements

The authors are thankful to the Botswana International University of Science and Technology (BIUST) for funding the research study through grant S100215.

## Authors' contributions

KB, GG, and TK formulated the design of the study. KB carried out the experiments and drafted the manuscript. PB performed the statistical analysis and revised the manuscript. GG and TK supervised the study and revised the manuscript. All authors read and approved the final manuscript.

## Compliance with ethical standards

**Conflict of interest:** Authors do not have any conflict of interests to declare.

**Ethical issues:** None.

## References

1. IDF. IDF diabetes atlas 10th edition [Internet]. Brussels, International Diabetes Federation. 2021; p. 5-7. <https://doi.org/https://diabetesatlas.org/atlas/tenth-edition/>
2. ElSayed NA, Aleppo G, Aroda VR, Bannuru RR, Brown FM, Bruemmer D *et al.* Classification and diagnosis of diabetes: Standards of care in diabetes. *Diabetes Care.* 2023;46(1):19-40. <https://doi.org/10.2337/dc23-S002>
3. Elsayed NA, Aleppo G, Aroda VR, Bannuru RR, Brown FM, Bruemmer D *et al.* Pharmacologic approaches to glycemic treatment: Standards of care in diabetes. *Diabetes Care.* 2023;46(suppl):S140-57. <https://doi.org/10.2337/dc23-S009>
4. Zhou X, Shrestha SS, Shao H, Zhang P. Factors contributing to the rising national cost of glucose lowering medicines for diabetes during 2005–2007 and 2015–2017. *Diabetes Care.* 2020;43(10):20-29. <https://doi.org/10.2337/dc19-2273>
5. Tiongco REG, Arceo ES, Rivera NS, Flake CCD, Policarpio AR. Estimation of salivary glucose, amylase, calcium and phosphorus among non-diabetics and diabetics: Potential identification of non-invasive diagnostic markers. *Diabetes Metab Syndr.* 2019;13(4):2601-05. <https://doi.org/10.1016/j.dsx.2019.07.037>
6. Pérez-Ros P, Navarro-Flores E, Julián-Rochina I, Martínez-Arnau FM, Cauli O. Changes in salivary amylase and glucose in diabetes: A scoping review. *Diagnostics.* 2021;11(3):453. <https://doi.org/10.3390/diagnostics11030453>
7. Standl E, Baumgartl HJ, Fuchtenbusch M, Stempler J. Effect of acarbose on additional insulin therapy in type 2 diabetic patients with late failure of sulphonylurea therapy. *Diabetes Obes Metab.* 1999;1(4):215-20. <https://doi.org/10.1046/j.1463-1326.1999.00021.x>
8. Kumar Y, Goyal K, Kumar AK. Pharmacotherapeutics of miglitol: An  $\alpha$ -glucosidase inhibitor. *J Anal Pharm Res.* 2018;7(6):617-19. <https://doi.org/10.15406/japlr.2018.07.00292>
9. Matsumoto K, Yano M, Miyake S, Ueki Y, Yamaguchi Y, Akazawa S, Tominaga Y. Effects of voglibose on glycemic excursions, insulin secretion and insulin sensitivity in non-insulin-treated NIDDM patients. *Diabetes Care.* 1998;21(2):256-60. <https://doi.org/10.2337/diacare.21.2.256>
10. Mentreddy SR. Medicinal plant species with potential antidiabetic properties. *J Sci Food Agric.* 2007;87(5):1074-79. <https://doi.org/10.1002/jsfa.2811>
11. Usai R, Majoni S, Rwere F. Natural products for the treatment and management of diabetes mellitus in Zimbabwe-a review. *Front Pharmacol.* 2022;13:1-21. <https://doi.org/10.3389/fphar.2022.980819>
12. Mbuni YM, Wang S, Mwangi BN, Mbari NJ, Musili PM, Walter NO, Hu G, Zhou Y, Wang Q. Medicinal plants and their traditional uses in local communities around Cherangani hills, Western Kenya. *Plants.* 2020;9(3):331. <https://doi.org/10.3390/plants9030331>
13. Renuka R, Jeyanthi GP. Evaluation of *in vitro*  $\alpha$ -amylase inhibitory kinetics and free radical scavenging activities of *Momordica charantia*. *Int J ChemTech Res.* 2017;10(7):315-23.
14. Li K, Yao F, Xue Q, Fan H, Yang L, Li X, Sun L, Liu Y. Inhibitory effects against  $\alpha$ -glucosidase and  $\alpha$ -amylase of the flavonoid-rich extract from *Scutellaria baicalensis* shoots and interpretation of structure–activity relationship of its eight flavonoids by a refined assign-score method. *Chem Cent J.* 2018;12(1):82. <https://doi.org/10.1186/s13065-018-0445-y>
15. Ben LJ, Boujbiha MA, Dahane S, Cherifa AB, Khlifi A, Chahdoura H *et al.*  $\alpha$ -Amylase and  $\alpha$ -glucosidase inhibitor effects and pancreatic response to diabetes mellitus on Wistar rats of Ephedra alata areal part decoction with immunohistochemical analyses. *Environ Sci Pollut Res.* 2019;26(10):9739-54. <https://doi.org/10.1007/s11356-019-04339-3>
16. Bati K, Kwape TE, Chaturvedi P. Anti-diabetic effects of an ethanol extract of *Cassia abbreviata* stem bark on diabetic rats and possible mechanism of its action. *J Pharmacopuncture.* 2017;20(1):45-51. <https://doi.org/10.3831/KPI.2017.20.008>
17. Maroyi A. Review of ethnomedicinal uses, phytochemistry and pharmacological properties of *Euclea natalensis* A.DC. *Molecules.* 2017;22(12):2128. <https://doi.org/10.3390/molecules22122128>
18. Lall N, Weiganand O, Hussein AA, Meyer JJM. Antifungal activity of naphthoquinones and triterpenes isolated from the root bark of *Euclea natalensis*. *S Afr J Bot.* 2006;72(4):579-83. <https://doi.org/10.1016/j.sajb.2006.03.005>
19. Kooy F, Meyer JJM, Lall N, Matumba MG, Ayeleso AO, Nyakudya TT *et al.* Antimycobacterial activity and possible mode of action of newly isolated neodiospyrin and other naphthoquinones from *Euclea natalensis*. *J Ethnopharmacol.* 2012;7:349-52. <https://doi.org/10.3390/molecules24040661>
20. Deutschländer MS, Lall N, Van de Venter M, Dewanjee S. The hypoglycemic activity of *Euclea undulata* Thunb. var. *myrtina* (Ebenaceae) root bark evaluated in a streptozotocin-nicotinamide induced type 2 diabetes rat model. *S Afr J Bot.* 2012;80:9-12. <https://doi.org/10.1016/j.sajb.2012.02.006>
21. Nkobole N, Houghton PJ, Hussein A, Lall N. Antidiabetic activity of *Terminalia sericea* constituents. *Nat Prod Commun.* 2011;6(11):1585-88. <https://doi.org/10.1177/1934578x1100601106>
22. Kamtekar S, Keer V, Patil V. Estimation of phenolic content, flavonoid content, antioxidant and alpha amylase inhibitory activity of marketed polyherbal formulation. *J Appl Pharm Sci.* 2014;4(9):61-65. <https://doi.org/10.7324/JAPS.2014.40911>

23. Dou F, Xi M, Wang J, Tian X, Hong L, Tang H, Wen A.  $\alpha$ -Glucosidase and  $\alpha$ -amylase inhibitory activities of saponins from traditional Chinese medicines in the treatment of diabetes mellitus. *Pharmazie*. 2013;68(4):300-04. <https://doi.org/10.1691/ph.2013.2753>
24. Bati K. Evaluation of the antidiabetic effects and possible mechanisms of action of *Euclea natalensis* extracts [Dissertation]. Botswana International University of Science and Technology; 2021.
25. Zhao B, Wu F, Han X, Zhou W, Shi Q, Wang H. Protective effects of acarbose against insulinitis in multiple low-dose streptozotocin-induced diabetic mice. *Life Sci*. 2020;263. <https://doi.org/10.1016/j.lfs.2020.118490>
26. Rosak C, Mertes G. Critical evaluation of the role of acarbose in the treatment of diabetes: Patient considerations. *Diabetes Metab Syndr Obes*. 2012;5:357-67. <https://doi.org/10.2147/dms.s28340>
27. Li W, Yuan G, Pan Y, Wang C, Chen H. Network pharmacology studies on the bioactive compounds and action mechanisms of natural products for the treatment of diabetes mellitus: A review. *Front Pharmacol*. 2017;8(2):1-10. <https://doi.org/10.3389/fphar.2017.00074>
28. Striegel L, Kang B, Pilkenton SJ, Rychlik M, Apostolidis E. Effect of black tea and black tea pomace polyphenols on  $\alpha$ -glucosidase and  $\alpha$ -amylase inhibition, relevant to type 2 diabetes prevention. *Front Nutr*. 2015;2(2):1-6. <https://doi.org/10.3389/fnut.2015.00003>
29. Deutschländer MS, Lall N, Van de Venter M, Hussein AA. Hypoglycemic evaluation of a new triterpene and other compounds isolated from *Euclea undulata* Thunb. var. *myrtina* (Ebenaceae) root bark. *J Ethnopharmacol*. 2011;133(3):1091-95. <https://doi.org/10.1016/J.JEP.2010.11.038>
30. Ali RB, Atangwho IJ, Kuar N, Ahmad M, Mahmud R, Asmawi MZ. *In vitro* and *in vivo* effects of standardized extract and fractions of *Phaleria macrocarpa* fruits pericarp on lead carbohydrate digesting enzymes. *BMC Complement Altern Med*. 2013;13:39. <https://doi.org/10.1186/1472-6882-13-39>
31. Guerrero-Romero F, Simental-Mendía LE, Guerra Rosas MI, Sayago-Monreal VI, Morales Castro J, Gamboa-Gómez CI. Hypoglycemic and antioxidant effects of green tomato (*Physalis ixocarpa* Brot.) calyces' extracts. *J Food Biochem*. 2021;45(4):e13678. <https://doi.org/10.1111/jfbc.13678>
32. Beejmohun V, Peytavy-Izard M, Mignon C, Muscente-Paque D, Deplanque X, Ripoll C, Chapal N. Acute effect of *Ceylon cinnamon* extract on postprandial glycemia: Alpha-amylase inhibition, starch tolerance test in rats and randomized crossover clinical trial in healthy volunteers. *BMC Complement Altern Med*. 2012;14(1):351. <https://doi.org/10.1186/1472-6882-14-351>
33. Meng XY, Zhang HX, Mezei M, Cui M. Molecular docking: A powerful approach for structure-based drug discovery. *Curr Comput Aided Drug Des*. 2012;7(2):146-57. <https://doi.org/10.2174/157340911795677602>
34. Li J, Fu A, Zhang L. An overview of scoring functions used for protein-ligand interactions in molecular docking. *Interdiscip Sci*. 2019;11(2):320-28. <https://doi.org/10.1007/s12539-019-00327-w>
35. Naqvi AAT, Mohammad T, Hasan GM, Hassan Mdl. Advances in docking and molecular dynamics simulations towards ligand-receptor interactions and structure-function relationships. *Curr Top Med Chem*. 2019;18(20):1755-68. <https://doi.org/10.2174/1568026618666181025114157>
36. Martínez L. Automatic identification of mobile and rigid substructures in molecular dynamics simulations and fractional structural fluctuation analysis. *PLoS One*. 2015;10(3):e0119264. <https://doi.org/10.1371/journal.pone.0119264>
37. Kwofie SK, Broni E, Asiedu SO, Kwarko GB, Dankwa B, Enniful KS *et al*. Cheminformatics-based identification of potential novel anti-sars-cov-2 natural compounds of African origin. *Molecules*. 2021;26(2):406. <https://doi.org/10.3390/molecules26020406>
38. Zhao Y, Zeng C, Massiah MA. Molecular dynamics simulation reveals insights into the mechanism of unfolding by the A130T/V mutations within the MID1 zinc-binding Bbox1 domain. *PLoS One*. 2015;10(4):e0124377. <https://doi.org/10.1371/journal.pone.0124377>
39. Oyewusi HA, Wu YS, Safi SZ, Wahab RA, Hatta MHM, Batumalaie K. Molecular dynamics simulations reveal the inhibitory mechanism of Withanolide A against  $\alpha$ -glucosidase and  $\alpha$ -amylase. *J Biomol Struct Dyn*. 2023;41(13):6203-18. <https://doi.org/10.1080/07391102.2022.2104375>
40. Akshatha JV, SantoshKumar HS, Prakash HS, Nalini MS. *In silico* docking studies of  $\alpha$ -amylase inhibitors from the anti-diabetic plant *Leucas ciliata* Benth. and an endophyte, *Streptomyces longisporoflavus*. *3Biotech*. 2021;11:51. <https://doi.org/10.1007/s13205-020-02547-0>
41. Swargiary A, Daimari M. GC-MS analysis of phytochemicals and antihyperglycemic property of *Hydrocotyle sibthorpioides* Lam. *SN Appl Sci*. 2021;3:36. <https://doi.org/10.1007/s42452-020-04101-2>